Dilute Poly(ethylene oxide) Aqueous Solutions in a Turbulent Flow

Michel Duval*,† and François Boué‡

Institut Charles Sadron (CNRS-ULP), 6 Rue Boussingault, 67083 Strasbourg Cedex, France, and Laboratoire Léon Brillouin UMR12, CNRS-CEA, Saclay 91191, Gif sur Yvette Cedex

Received October 19, 2006; Revised Manuscript Received August 30, 2007

ABSTRACT: After successive passes through a syringe needle, poly(ethylene oxide) (PEO) in dilute aqueous solution undergoes chain aggregation. The degree of association, the size, and the concentration of the species are characterized by combining static and dynamic light scattering measurements. For the highest molecular weight, polymer chains are broken in a first stage then aggregate in a second stage. Neutron scattering results show that these chains have the same conformation as in the dispersed molecular state. When the solutions are allowed to rest, the aggregates dissociate very slowly with time. After addition of sodium chloride, the dissociation is much faster and complete. We propose the aggregation to result from the concomitant increase of the instantaneous local concentration at the entrance of the syringe needle and the enhanced hydrophobic interactions to which are submitted the stretched macromolecular chains in the flow.

Introduction

The ability of poly(ethylene oxide) (PEO) to reduce frictional drag in the turbulent flow of fluids is well-known. However this phenomenon is considerably restricted by the fact that the polymer undergoes rapid degradations in the flow field due to the high shear field associated with the turbulences. Many authors have studied this reduction of frictional drag not only on PEO solutions[1−6] but also on other polymer solutions.[1,2,5,6] In the dilute concentration regime, entanglements between polymer chains are not present so they cannot produce any stress resulting in degradation, which rather should come from the friction forces on the chains. Indeed intense velocity gradients exist in the boundary layer near the walls of the pipe. This can lead to the development of tensile forces on the molecules and provides a mechanical activation energy for chain scission of polymer molecules. Thus the polymer chains could be completely extended along the streamlines of flow and subsequently cut.

This paper reports some different effects of a flow on dilute aqueous PEO solutions when passing through the needle (1 mm diameter) of a syringe. Four PEO samples are studied with molecular weights going from $M_w \cong 6000$ Da to $M_w \cong 2 \times 10^6$ Da. The polymer solutions are studied by combining static (SLS) and dynamic (DLS) light scattering results and small angle neutron scattering (SANS) measurements. The objects, made of polymer chains, present in the medium are characterized by the concentration (C), the average molecular weight (M_w), the average radius of gyration (R_{GZ}), and the distribution function of the hydrodynamic radius (R_H). The effect of the number of passes through the needle and of the nature of the solvent are studied. After processing the solutions, aging is followed as well as the effect of the addition of salt.

Experimental Section

Materials. All the solvents used in this study are spectroscopic purity grade products. Freshly tridistilled water is used to prepare aqueous PEO solutions. Deuterium oxide (99.9% D) is obtained from CEA (Euriso-Top, Saclay, France). All measurements are performed at 25 °C. The low molecular weight samples (PEO6 and PEO20) are purchased from Fluka Co.; the high molecular weight samples (PEO300 and PEO2000) are purchased from Aldrich Co. The characteristics of the samples are listed in Table 1. It should be noted that the experimental values of the molecular weight measured by gel permeation chromatography for PEO6 and PEO20 are somewhat higher than the measured values by light scattering that, however, are in better agreement with the values given by Fluka. The accuracy of the measurements in the static light scattering experiments is generally estimated to 8−10%.[7] The accuracy on the R_H values is estimated to 5%. The samples are characterized in three different solvents namely tridistilled water, tridistilled water + sodium chloride (NaCl, 1 N), and methanol. This point is very important in the case where former history of the commercial sample is not known: it is then essential to be sure that the polymer does not contain aggregates[8] from the beginning. In Table 1, the increase of the viscosity of the NaCl 1 N solution as compared to water has not been taken into account for the calculation of R_H.

Preparation of the Solutions. The preparation of the aqueous PEO solutions for light scattering studies requires great care: dust and solid particles must be absent, chains must be perfectly dissolved, and at the same time one must avoid degradations of any sort, either mechanical or chemical. All the solutions are prepared gravimetrically. At first they are maintained in an oven for 6 h at 55 °C. Then they are gently shaken in a dark room at 22 °C for 12 h. No magnetic stirrer is used to avoid breakdown of the polymer chains. They are put again in the oven at 55 °C for 6 h and again agitated in the dark for 12 h. The solutions of lower concentration are made from stock solutions by dilution. The optical clarification of the solutions is carried out by filtering slowly without any pressure directly into the light scattering cells through 0.45 μm (nominal pore size) polytetrafluoroethylene (hydrophilic PTFE) filters from Millipore Co. Before any experimental process on the PEO solutions, the absence of dust and aggregated chains is checked by measurement of the correlation function of the scattered intensity where only one sharp relaxation mode is observed.

Method

Sixteen milliliters of aqueous PEO solutions are put in a closed 50 mL flask connected to a 5 mL syringe via a needle (diameter, 1 mm; length, 11 cm). The solution is slowly pumped in the syringe and then vigorously pumped out back into the flask under a pressure of 4.5 atm exerted by the piston. This process is repeated as many times as required. Then the solutions are filtered directly into the scattering cells as mentioned above.

* Corresponding author. E-mail: Duval@ics.u-strasbg.fr.
† Institut Charles Sadron (CNRS-ULP).
‡ Laboratoire Léon Brillouin UMR12, CNRS-CEA.

10.1021/ma062411r CCC: $37.00
Published on Web 10/18/2007

Table 1. Properties of PEO Samples

sample	PEO6	PEO20	PEO300	PEO2000
M_w (kDa)[a]	7.4	24	490	2130
polydispersity index[a]	1.02	1.06	1.42	2.60
M_w (kDa)[b]	6.0, 6.6, 6.5	19, 20, 20	530, 480, 450	1700, 1980, 2200
$A_2 \times 10^3$ (cm^3 mol g^{-2})[b]	2.0, 3.4, 3.8	1.4, 2.3, 2.7	0.9, 0.5, 0.7	0.6, 0.7, 1.0
R_G (nm)[b]	3.0[c]		61, 59, 58	122, 125, 142
R_H (nm)[b]	2.2, 2.5, 2.4	4.2, 4.7, 4.9	32, 39, 40	73, 81, 85

[a] Measured by gel permeation chromatography in tridistilled water (0.1 N $NaNO_3$). [b] Measured by SLS and DLS in methanol, tridistilled water, and tridistilled water (1 N NaCl), respectively. [c] Measured by neutron scattering in D_2O.

Light Scattering Measurement. The static (SLS) and dynamic (DLS) light scattering measurements are performed in the angular range $22° < \theta < 145°$ using the ALV/DLS/SLS-5020F experimental setup (ALV-Laser Vertriebsgesellshaft mbH, Langen, Germany) consisting of an He−Ne laser (22 mW, $\lambda_0 = 632.8$ nm), a compact ALV/CGS-8 goniometer system, and an ALV-5000 autocorrelator. This angular range corresponds to scattering vectors q between 5×10^{-4} and 2.5×10^{-3} Å^{-1} where q is given by

$$q = 4\frac{\pi}{\lambda_0} n \sin(\theta/2) \tag{1}$$

n being the solvent refractive index and λ_0 the wavelength of the incident light in vacuum. The values of the absolute scattering cross section $I(q)$, in cm^{-1}, are obtained through the calibration with a toluene standard (Rayleigh ratio $= 1.368 \times 10^{-5}$ cm^{-1}). In SLS, the angular dependence of the excess absolute time-averaged scattered intensity $R(q)$ is related, in the case of a Gaussian distribution of the statistical segments of the macromolecular chains, to the weight-average molecular weight, M_w, the second virial coefficient A_2, and the z-average radius of gyration $\langle R_G^2\rangle_z^{1/2}$ by[9]

$$\frac{KC}{R(q)} = \frac{1}{M_w}\left(1 + \frac{1}{3}q^2\langle R_G{}^2\rangle_z\right) + 2A_2C \tag{2}$$

where $K = 4\pi^2 n^2 (dn/dC)^2/(N_A\lambda_0^4)$ with N_A being Avogadro's constant and C the polymer concentration. The refractive index increments (dn/dC) of aqueous PEO solutions added with salt are measured as a function of the NaCl concentration (C_{NaCl} in g cm^{-3}) on a Brice−Phoenix differential refractometer. The following empirical law is obtained

$$\frac{dn}{dC} = 0.133 - 0.156C_{NaCl} \tag{3}$$

In the case of a mixture of monodisperse species consisting of aggregates of molecular weight M_{wag} and individual chains of molecular weight M_{wextch}, which we call external because they do not belong to the aggregates, the apparent molecular weight measured by light scattering is given by

$$M_{wapp} = x_{extch}M_{wextch} + (1 - x_{extch})M_{wag} \tag{4}$$

x_{extch} being the weight fraction of the nonaggregated species. In the approximation of a Gaussian distribution of the segments, the apparent radius of gyration is given by

$$\langle R_{Gapp}{}^2\rangle_z = y\langle R_{Gextch}{}^2\rangle_z + (1 - y)\langle R_{Gag}{}^2\rangle_z \tag{5}$$

with $y = x_{extch}M_{wextch}/M_{wapp}$.

The normalized autocorrelation functions $g^{(2)}(q,t)$ of the scattered light are analyzed using the CONTIN routine[10] built in the ALV software following the relationship[11]

$$g^{(2)}(q,t) = 1 + [\beta\int \exp(-t/\tau)G(\tau)d\tau]^2 \tag{6}$$

where t is the time, $G(\tau)$ is the distribution function of the relaxation times τ, and $\beta \approx 1$ is the coherence factor of the instrument. The hydrodynamic radius R_H of the scattering species, which is proportional to the inverse of the z-average diffusion coefficient ($\langle D\rangle_z$), is calculated through the Stokes−Einstein relationship:[12]

$$R_H = q^2\frac{k_BT}{6\pi\eta_0}\tau(q) \tag{7}$$

where k_B is the Boltzmann constant, T the absolute temperature, and η_0 the viscosity of the solvent. The peak area in $G(\tau)$ is proportional to the excess scattered intensity. It has been shown that, in the case of a mixture of individual and aggregated chains, a combination of SLS and DLS results can provide information on the aggregation number as well as the weight fraction of the aggregates in the solution.[13−15] When the two scattering species have very different molecular weights, the CONTIN analysis of the correlation functions of the scattered light gives two peaks and the area ratio A of these two peaks is given by

$$A = \frac{A_{extch}}{A_{ag}} = \frac{M^*_{wextch}C_{extch}}{M^*_{wag}C_{ag}} \tag{8}$$

where M^*_{wextch} and M^*_{wag} are the apparent weight-average molecular weight at finite concentration C_{extch} and C_{ag}. Extrapolated to zero concentration, this relation gives

$$A^{q\to0}_{C\to0} = \frac{x_{extch}M_{wextch}}{(1 - x_{extch})M_{wag}} \tag{9}$$

If we know M_{wapp},measured by SLS, and the ratio $A^{q\to0}_{C\to0}$, measured by DLS, we have access to the quantities $x_{extch}M_{wextch}$ and $(1 - x_{extch})M_{wag}$ using eqs 4 and 9. Since the molecular weight M_{wextch} of the individual chains in the mixture is known, provided the polymer is not degraded during the processing, we can deduce x_{extch} and hence M_{wag}. There are however some limitations to this reasoning. The first one is practical: if the aggregates are very large, they dominate largely the scattering at low q such that it becomes very difficult to estimate the contribution "$x_{extch}M_{extch}$"; it is negligible if the sum (4) and the ratio (9) are too small to be correctly measured. We then lose the information about x_{extch} and hence on x_{ag} and know only the product $x_{ag}M_{wag}$. The second limitation is physical: we have noticed that the fast mode is mostly due to free individual chains whereas it can come from the inside of the aggregates if they are not compact but on the contrary contain a lot of water. Then the inner chains may scatter as well as the external one, and the two contributions merge in the fast mode. It is actually impossible to distinguish the two situations.

Neutron Scattering Measurement. The neutron scattering experiments are performed on the spectrometer PACE at Laboratoire Léon Brillouin, Saclay (France), in the range $3.4 \times 10^{-3} \le q(Å^{-1}) \le 4.3 \times 10^{-1}$. Three setups are used corresponding to sample−detector distance $D = 4$, 3.2, and 1 m at three different wavelengths $\lambda = 12$, 6, and 4 Å. The collimation is mostly obtained by diaphragms of diameter 12 mm at 4 m, 16 mm at 3.2 m, and 22 mm at 1 m. All intensities are corrected by transmission and then subtracted from empty cell scattering. Detector efficiency is corrected by dividing these intensities by the scattering from 1 mm water (minus empty cell scattering). These intensities are then multiplied by the water absolute scattering section which is directly measured (respectively, 1.4, 1, and 0.9 cm^{-1} at 12, 6, and 4 Å).

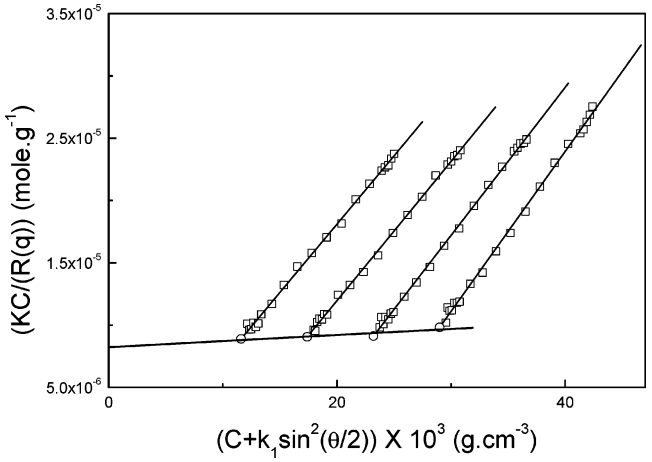

Figure 1. Typical Zimm plot for PEO6 after that the aqueous solution at $C = 2.9 \times 10^{-2}$ g cm^{-3} is passed 900 times through the syringe needle.

Table 2. Characteristics of PEO Samples after the Aqueous Solutions Are Passed 900 Times through the Syringe Needle

sample	M_w (kDa)	$A_2 \times 10^5$ (cm^3 mol g^{-2})	R_G (nm)	R_H (nm)
PEO6	142	5	93	111
PEO20	165	−6	79	103
PEO300	1500	−3.7	80	74
PEO2000	5700	−1.2	104	98

Incoherent background is subtracted using the scattering of pure D_2O plus the 3% contribution of the polymer itself. For processed samples, an extra incoherent scattering of a few percent of D_2O scattering has to be removed. It probably corresponds to a small amount of nondeuterated water due to exchange with the air during processing.

Results and Discussion

Figure 1 shows a typical Zimm plot of static light scattering from a PEO6 aqueous solution ($C = 2.9 \times 10^{-2}$ g cm^{-3}) that is passed 900 times through the syringe needle. It can be noted on this plot that the inverse of the scattered light is q^2 linearly dependent (no curvature is observed). From the light scattering cross-section extrapolated to zero concentration, we can calculate the molecular weight (called above M_{wapp}) by extrapolation at the zero angle (first line of Table 2); we see that it is much higher than before processing. For the same function, the slope of the lines $1/R = f(q^2)$ yields a value of the radius of gyration of the scattering entities (93 nm in Table 2) which is very large compared to the value expected for chains of 7000 Da. We also see that the apparent second virial coefficient (slope of the line $1/R_{q=0} = f(C)$) for these objects is low, of order 10^{-5}, compared to 10^{-3} for nonprocessed chains (Table 1). Figure 2 shows the distribution function of the hydrodynamic radius of the scattering particles at $C = 2.9 \times 10^{-2}$ g cm^{-3} and $\theta = 30°$ before and after the processing through the syringe needle as measured by DLS. We observe that a new value of R_H appears, much larger than the R_H value of the individual chain. Remarkably the corresponding peak is 20 times higher and also wider. As said above, the peak area in $G(\tau)$ (or here $G(R_H)$) is proportional to the excess scattered intensity which is then very much larger than the intensity scattered by individual chains. These remarks on SLS and DLS results apply to all samples under investigation as shown by Table 2 for the four PEO samples submitted to the process. However, the single chain and aggregate dimensions are close in the case of samples PEO300 and PEO2000.

Let us compare R_G and R_H values. We must keep in mind that, since the R_G values are *z*-average values while the R_H values

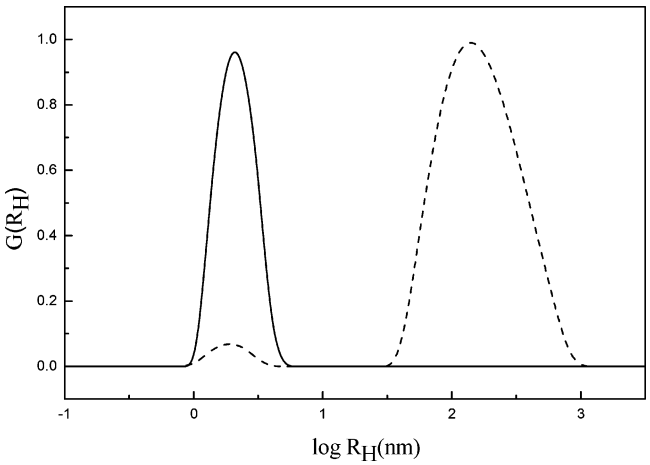

Figure 2. Distribution function $G(R_H)$ of the hydrodynamic radius of PEO6 at $C = 2.9 \times 10^{-2}$ g cm^{-3} and $\theta = 30°$. Solid line, original solution; dashed line, after processing (900 passes).

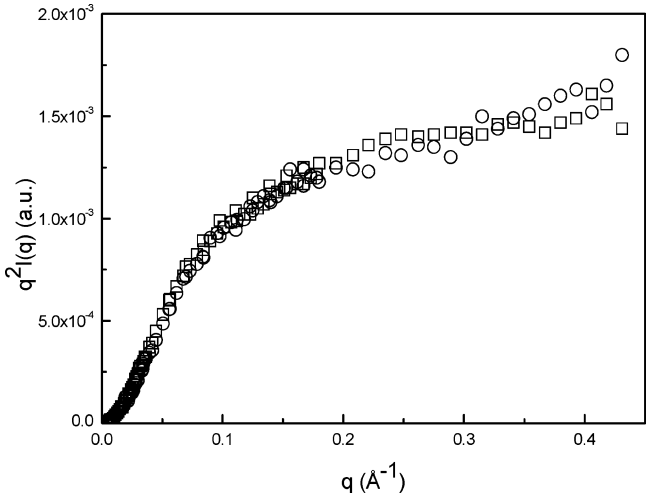

Figure 3. Wave vector dependence of the neutron scattered intensity for the original (□) and processed (○) PEO6 in D_2O at $C = 2.9 \times 10^{-2}$ g cm^{-3}.

are taken at the maximum of the distribution curves $G(R_H)$, their ratio depends on the polydispersity which is high for aggregates compared to the initial PEO molecules (see Figure 2). In spite of that, the values of the ratio R_G/R_H are low ($0.77 < R_G/R_H < 1.08$); this indicates that the aggregates are globular structures (we recall that the value of this ratio varies from 0.77 for a compact sphere to 1.51 for a Gaussian coil and 1.86 for a coil with excluded volume).[16] Taking into account the dimensions of these objects with respect to their apparent molecular weights, we can infer that they are not very dense.

Structure of the PEO Aggregates. Since the objects are not dense, the inner chain−solvent mixture inside the aggregates can scatter radiation as well as external chains. In order to observe their corresponding scattering, which will correspond to a lower spatial scale, neutron scattering measurements (SANS) are performed on processed (900 passes) PEO6 solutions in D_2O. It should be noted that the behavior of PEO in H_2O and in D_2O could be slightly different, before going any further. However, light scattering measurements on PEO6/D_2O processed solutions ($M_w = 90\,000$ Da; $A_2 = 2 \times 10^{-5}$ cm^3 mol g^{-2}; $R_G = 78$ nm; $R_H = 99$ nm) give results which are not far from those of the PEO6/H_2O processed solutions (see line 1 of Table 2).

Figure 3 compares the SANS signal given by the original and the processed samples in a $q^2I(q)$ vs q Kratky representation.

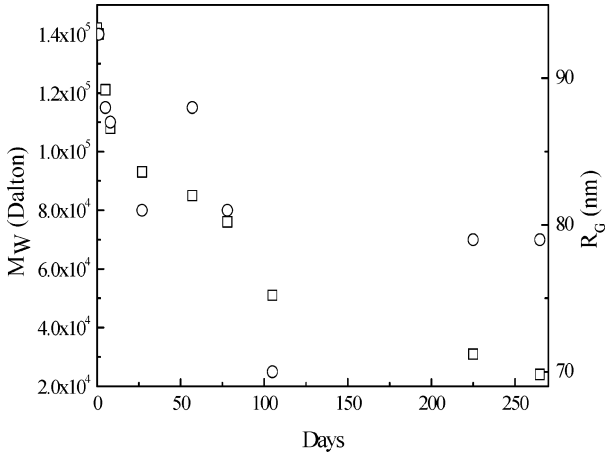

Figure 4. Aging of the aggregates of PEO6 aqueous solutions. Variation of the molecular weight □ and of the radius of gyration ○ as a function of time.

This representation is very sensitive to any deviation of chain conformation from the Gaussian conformation. The two signals can be totally superposed without any front factor adjustment. This is also true using any other representation (like the log−log one) in particular at low q values. In other words, it appears that the signal from the PEO chains has not changed. It can be deduced that their conformations inside the aggregates are identical to the conformation of the individual chains. It should be noted that we also observe the same q dependence for processed and nonprocessed solutions of high molecular weight chains (PEO2000 at $C = 10^{-4}$ g cm^{-3}) the accuracy of the measurement being reduced in such a low concentration range. In conclusion, we propose that the aggregates are loose assemblies of short chains which scatter as individual ones. On top of their scattering which remains unchanged, build up some aggregate scattering gives a much larger contribution.

Aging of the PEO Aggregates. The PEO6 aqueous solution processed through the needle of the syringe is kept in the dark at 22 °C, and the aging of the solution is followed by performing periodic SLS measurements. The results of Figure 4 show a slow dissociation of the chain aggregates with time. After 3 months, the molecular weight of the scattering species has decreased by a factor 3 and the radius of gyration has decreased from 93 to 70 nm. There still remains aggregates after 8 months of aging. Let us remark that this slow dissociation of the aggregates can be speeded up under the influence of external forces. It can well explain the fact that aggregates are not detected by GPC measurements, which impose rather strong shear stress inside the column.

Salt Induced Dissociation of the PEO Aggregates. The effect of salt addition is also studied. Polik and Burchard[17] have ascribed chain aggregation in aqueous solutions to hydrophobic interactions via the increase in the ordering of water molecules in the vicinity of PEO. The addition of salt should dismantle the structure of these solutions. The characteristics of processed PEO aqueous solutions after addition of NaCl (1 N) as measured by SLS and DLS are given in Table 3. The physical parameters of the initial samples are recovered for the low molecular weight samples (PEO6, PEO20, and PEO300). Conversely, the molecular weight of PEO2000 has dropped down from 2 130 000 to 528 000 Da. This can be explained by the fact that, before, to aggregate, long chains are broken by the flow gradients.

It is interesting to check whether breaking of the chains occurs initially without further permanent alteration of individual chains or not. Since long chains are more sensitive to any alteration,

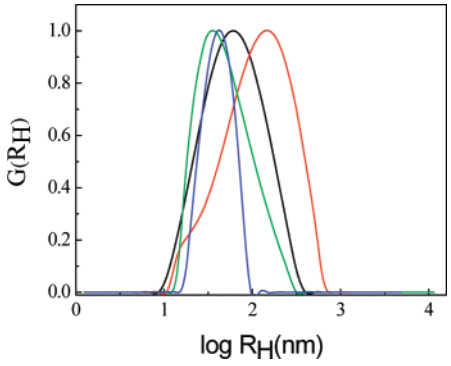

Figure 5. Distribution function $G(R_H)$ of the hydrodynamic radius of PEO2000 in aqueous solution at $C = 7.5 \times 10^{-4}$g cm^{-3} (scattering angle 30°): (black line) initial solution; (red line) after processing; (blue line) after processing and addition of NaCl (1 N); (green line) after processing, addition of NaCl (1 N), and dialysis.

Table 3. Characteristics of PEO Samples after the Processing of the Aqueous Solutions (900 Passages through the Syringe Needle) and after Addition of 1 N NaCl

sample	M_w (kDa)	$A_2 \times 10^3$ (cm^3 mol g^{-2})	R_G (nm)	R_H (nm)
PEO6	6	1.5		2.2
PEO20	20	1.3		4.4
PEO300	451	0.7	58	36
PEO2000	528	0.4	49	35

PEO2000 chains are chosen; an aqueous solution is prepared and processed 100 times through the syringe needle. Then NaCl (1 N) is added in order to dissolve the aggregates and is removed by dialysis. The distribution functions of the hydrodynamic radius given by the CONTIN analysis of the correlation function of the scattered intensity measured by DLS at each stage of the experiment are shown in Figure 5.

These values are apparent values since they are performed at finite concentration. Nevertheless they display the same behavior as real extrapolations: the aggregation of the PEO molecules can be observed during the process since the average R_H value increases from 61 to 112 nm. The distribution function is large. The addition of NaCl breaks the aggregates: the average R_H value decreases to 46 nm, of the order of the initial value. Finally it can be noted that, after dialysis of the solution, the PEO chains remain dispersed and no spontaneous aggregation occurs. The processing tightens the distribution since the large chains are the most easily degraded by the flow.

Effect of the Nature of the Solvent. Experiments in other solvents show that the aggregation behavior of PEO is specific to aqueous solutions. The four samples under investigation are dissolved in water 1 N NaCl, in methanol, in allyl alcohol, and in dioxane. The solutions are submitted to the same treatment as for the aqueous solutions. In these solvents it is again observed that large chains are broken as in aqueous solution. However, for the four samples under investigation, there is no aggregation. The specific interactions between the molecules of water and the PEO chains have a major influence on the formation of the aggregates.

Effect of the Number of Processing through the Syringe Needle. In order to follow the evolution of aggregation, during the process simultaneous SLS and DLS measurements are performed on PEO6 aqueous solutions which are processed 100 times and 300 times through the syringe needle. The solutions are characterized by the weight fraction x_{ag} and the molecular weight M_{wag} of the aggregates. Figure 6 shows a typical Zimm plot obtained for 100 processing.

The shape of the scattering curves reveals the presence of several scattering species in the solution. This is confirmed by

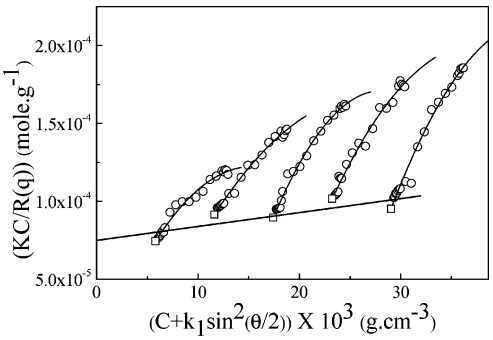

Figure 6. Zimm plot for PEO6 after the aqueous solution at $C = 2.9 \times 10^{-2}$ g cm^{-3} is passed 100 times through the syringe needle.

Table 4. Characteristics of PEO6 Aqueous Solutions as a Function of the Number of Processings through the Syringe Needle

number of processings	100	300	900
M_w^{app} (kDa)[a]	11.4	39	142
$A_2^{app} \times 10^4$ (cm^3 mol g^{-2})[a]	4.2	2.1	0.5
R_G^{app} (nm)[a]	53	67	93
M_{wag} (kDa)[b]	42	242	
R_{Gag} (nm)[c]	55	68	
R_{Hextch} (nm)[d]	2.4	2.4	
R_{Hag} (nm)[d]	77	62	111
x_{ag} (%)[b]	15	14	

[a] Measured by SLS. [b] Calculated from eqs 4 and eq 9. [c] Calculated from eq 5. [d] Measured by DLS.

DLS measurements which lead to a bimodal distribution of the hydrodynamic radii. The scattering curves given by the solutions that are processed 300 times are straight lines as in the case of the 900 times processed solutions (see Figure 1) but the DLS spectra show clearly a bimodal distribution of the hydrodynamic radius. The distribution functions of the hydrodynamic radius of the large species are broad showing that the aggregates are polydisperse. Nevertheless, we give an approximated calculation of the composition of the solutions in isolated and aggregated structure using the combination of the SLS and DLS results with respect to eqs 4, 5, 8, and 9. As said above, this relies on the absence of fast mode/large q scattering from chains inside the aggregates which is the major approximation of the method used. The physical parameters that characterize the polymer solutions are given in Table 4 where the results of the previous measurements (900 times) are recalled.

For number of passes lower than 900, one can observe that the apparent molecular weight, the apparent radius of gyration, and the molecular weight of the aggregates M_{wag} increase with the number of processings through the syringe needle. As found in the previous experiment, the radii of gyration R_{Gag} of the aggregates are high as compared to the values of their molecular weight. The apparent second virial coefficient decreases as the molecular weight of the aggregates increases. The hydrodynamic radius R_{Hextch} of the low molecular weight scattering species is equal to the hydrodynamic radius of the isolated PEO6 molecules. The hydrodynamic radius R_{Hag} of the large species are of the order of magnitude of the radius of gyration, and taking account of the remark made previously connected with the polydispersity of the scattering entities, this shows that the aggregates have a globular structure. Finally the estimated weight fraction of aggregates x_{ag} is the same for 100 and 300 passes, so it seems to be independent of the number of processing in this range at least. In the experiment involving 900 processes through the syringe needle, the scattered light signal is mainly due to the large aggregates. The distribution functions of the relaxation times are bimodal but the amplitudes of the slow relaxation times are so high (see Figure 2) that one cannot get a satisfactory accuracy in the analysis of the scattering spectra.

Conclusion

In this work, the behavior of macromolecular chains of PEO is studied in aqueous solutions when they are submitted to a turbulent flow. It is shown that these solutions have specific behavior that does not exist in other solvents. In the first stage, the large PEO chains are broken. Then, whatever the size of these chains, they form aggregates. In the conditions chosen for the applied stress at the syringe entrance, until 300 passes, the weight fraction of these aggregates grows up to 15% regardless of the time the stress is applied unlike the degree of association that increases with time. Under thermal entropic motion exclusively, at room temperature ($T = 22$ °C), the aggregates break up very slowly with time. The neutron and light scattering measurements show that the associated chains have the same conformation as the well solvated chains in water and that the aggregates have a globular structure. The addition of salt to the solutions leads in a few hours to the dismantling of the aggregates and isolated chains are recovered. This supports the idea that the formation of these aggregates is ascribed to the presence of hydrophobic interactions. Indeed these hydrophobic interactions between the CH_2 groups and the water molecules are enhanced under the cumulative effect of the stretched conformation of the chains and possibly an increase of the instantaneous local concentration of the polymeric chains in the turbulent flow.

Acknowledgment. We thank for valuable discussions F. Schosseler and M. Rawiso with whom we also performed the neutron measurements. We thank Laboratoire Léon Brillouin for the measurements on PACE.

Supporting Information Available: Additional Zimm plots and plot of correlation function for PEO6 at $C = 2.3 \times 10^{-2}$ g cm^{-3}. This material is available free of charge via the Internet at http://pubs.acs.org.

References and Notes

(1) Brennen, C.; Gadd, G. E. *Nature* **1967**, *215*, 1368−1370.
(2) Laufer, Z.; Jalink, H. L.; Staverman, J. *J. Polym. Sci., Polym. Chem. Ed.* **1973**, *11*, 3005−3015.
(3) Ting, R. Y.; Little, R. C. *J. Appl. Polym. Sci.* **1973**, *17*, 3345−3356.
(4) Cox, L. R.; Dunlop, E. H.; North, A. M. *Nature* **1974**, *249*, 243−245.
(5) Buchholz, F. L.; Wilson, L. R. *J. Appl. Polym. Sci.* **1986**, *32*, 5399−5413.
(6) D'Almeida, A. R.; Dias, M. L. *Polym. Degrad. Stab.* **1997**, *56*, 331−337.
(7) Huglin, M. B. *Light Scattering from Polymer Solutions*; Academic Press: London and New York, 1972.
(8) Duval, M.; Sarazin, D. *Macromolecules* **2003**, *36*, 1318−1323.
(9) Zimm, B. H. *J. Chem. Phys.* **1948**, *16*, 1099−1116.
(10) Provencher, S. W. *Comput. Phys. Commun.* **1982**, *27*, 229−242.
(11) Berne, B.; Pecora, R. *Dynamic Light Scattering with Applications to Chemistry, Biology and Physics*; Wiley-Interscience: New York, 1976.
(12) Yamakawa, H. *Modern Theory of Polymer Solutions*; Harper & Row: New York, 1971.
(13) Zhou, Z.; Peiffer, D. G.; Chu, B. *Macromolecules* **1994**, *27*, 1428−1433.
(14) Raspaud, E.; Lairez, D.; Adam, M.; Carton, J. P. *Macromolecules* **1994**, *27*, 2956−2964.
(15) Klucker, R.; Munch, J. P.; Schosseler, F. *Macromolecules* **1997**, *30*, 3839−3848.
(16) Akcasu, A. Z.; Han, C. C. *Macromolecules* **1979**, *12*, 276−280.
(17) Polik, F. W.; Burchard, W. *Macromolecules* **1983**, *16*, 978−982.

MA062411R